

# Nontrivial Ground State Degeneracy of the Spin–Pseudospin Model of a Two-Dimensional Magnet Near the Frustration Point

D. N. Yasinskaya<sup>\*1</sup>, V. A. Ulitko<sup>1</sup>, Yu. D. Panov<sup>1</sup>

<sup>1</sup>Ural Federal University 620002, 19 Mira Street, Ekaterinburg, Russia

\*daria.iasinskaia@urfu.ru

The classical Monte Carlo method is used to study the properties of the ground state and phase transitions of the spin–pseudospin model, which describes a two-dimensional Ising magnet with competing charge and spin interactions. This competition leads to the ground state degeneracy and the frustration of the system. It is shown that the ground state degeneracy is observed in the frustration area with nonzero probabilities of the formation of two different ordered states. Based on the histogram analysis of the Monte Carlo data, the type of phase transitions is analyzed. It is found that, near the frustration point, first-order phase transitions are observed in the dependence on the ratio between the spin ( $s = 1/2$ ) and pseudospin ( $S = 1$ ) interactions.

**Keywords:** dilute Ising magnet, frustration, Monte Carlo method, ground state, phase transitions

## 1 Introduction

The problem of elucidation of the microscopic nature of unusual properties of systems with strong interparticle interactions becomes more complex as there is competition and/or coexistence of various types of ordering. This problem is topical for hightemperature superconducting (HTSC) cuprates in which the static magnetic order and the charge density waves coexist [1]. The systems with various degrees of freedom are usually described using pseudospin models [2, 3].

The spin–pseudospin model considered in this work was proposed in [4] for studying the competition of the charge (related to pseudospin) and spin degrees of freedom in a quasi-two-dimensional HTSC cuprate in the normal state. This model, like many other pseudospin models, is also suited to the description of physical properties of dilute frustrated magnets. Due to the flexibility in the definition of the physical meaning of pseudospin operators, pseudospin models are widely used for describing the properties of a great variety of physical systems. An example is the known Blume–Emery–Griffiths model [5], which is used for the description of properties of binary alloys [6], multicomponent liquids and dilute magnets [7], and also cold atoms and superconducting systems [8, 9]. Even simple lattice models, such as the Ising or Potts models can describe a wide class of real physical systems in the dependence on the physical meaning of pseudospins [10].

The competition between charge (pseudospin) and magnetic (spin) orderings in the system under study leads to the system frustration. The systems with two and more competing interactions, each of which leads to a certain type of ordering, have a wide variety of ordered phase states with various thermodynamic properties and complex symmetry. In addition, the frustrated systems have a high sensitivity to external influences, fields, anisotropy, and impurities [10, 11] and demonstrate changes in the critical behavior [12]. Moreover, the models of frustrated magnets are interesting for their close connection with spin liquids, glasses [13], and ices [14].

## 2 Model and Methods

The spin–pseudospin model [4] is a system of mixed type with spin  $s = 1/2$  and pseudospin  $S = 1$ . We use pseudospin to describe valence states of the  $\text{CuO}_2$  planes of HTSC  $\text{La}_{2-x}\text{Sr}_x\text{CuO}_4$  cuprates in the framework of the pseudospin formalism. Here, pseudospin  $S = 1$  is a “charge triplet” related to three stable valence states of  $[\text{CuO}_4]^{5-,6-,7-}$  centers in the  $\text{CuO}_2$  plane. Pseudospin projections  $S_z = \pm 1$  are related to two nonmagnetic centers  $[\text{CuO}_4]^{5-,7-}$  with spin 0 in the ground state.

The magnetic state  $[\text{CuO}_4]^{6-}$  is related to pseudospin projection  $S_z = 0$  and is a spin doublet with  $s = 1/2$ . Thus, every site of a two-dimensional lattice can be in two charge states related to pseudospin projections  $S_z = \pm 1$  and in two spin states related to two spin projections  $s_z = \pm 1/2$ .

The Hamiltonian of the spin–pseudospin model of a magnet includes the single-ion pseudospin anisotropy  $\Delta$ , pseudospin Ising exchange interaction  $V$ , and also the conventional spin exchange interaction in the Ising form  $J$ :

$$\mathcal{H} = \Delta \sum_i S_{iz}^2 + V \sum_{\langle ij \rangle} S_{iz} S_{jz} + \tilde{J} \sum_{\langle ij \rangle} \sigma_{iz} \sigma_{jz} - \mu \sum_i S_{iz}. \quad (1)$$

The summation is carried out over  $N$  sites of a two-dimensional square lattice, and  $\langle ij \rangle$  denotes the nearest neighbors. Here  $\sigma_{iz} = P_{0i} s_{iz} / s$  is the normalized  $z$ -component of spin  $s = 1/2$  multiplied by projection operator  $P_{0i} = 1 - S_{iz}^2$ , which selects the magnetic  $[\text{CuO}_4]^{6-}$  state with  $S_z = 0$ ,  $\tilde{J} = Js^2 = J/4$ , and  $\mu$  is the chemical potential necessary to take into account the condition of the charge constancy:

$$n = \frac{1}{N} \sum_i S_{iz} = \text{const}, \quad (2)$$

where  $n$  is the charge density counted from the charge of the  $[\text{CuO}_4]^{6-}$ -center.

The “interaction” and the competition between charge and spin orderings in this model are due to kinematic restrictions related to the condition of the completeness of the set of possible states at a given lattice site: the spin doublet with  $S_z = 0$  and  $s_z = \pm 1/2$  and the charge doublet with  $S_z = \pm 1$  and  $s = 0$ . In Hamiltonian (1), this correlation is taken into account in the explicit form in projection operator  $P_0$  entering in  $\sigma_z$ , where it acts as the spin density operator for the  $[\text{CuO}_4]^{6-}$ -centers.

In addition, we note that charge–charge interaction  $\hat{V}$  of quite general form can be reduced to Hamiltonian (1) in the point charge approximation. Using the projectors for various valence states of the  $\text{CuO}_4$  center:  $P_1$  for  $[\text{CuO}_4]^{5-}$ ,  $P_0$  for

$[\text{CuO}_4]^{6-}$ , and  $P_{-1}$  for  $[\text{CuO}_4]^{7-}$ , we write

$$\hat{V} = \sum_{\langle ij \rangle} \sum_{a,b} V_{ab} P_{ia} P_{jb}.$$

Assuming that for the nearest neighbors on a square lattice  $V_{ab} = V q_a q_b$ , where  $q_0$  is a charge of a center  $[\text{CuO}_4]^{6-}$ ,  $q_1 = q_0 + 1$  and  $q_{-1} = q_0 - 1$  are the charges of centers  $[\text{CuO}_4]^{5-}$  and  $[\text{CuO}_4]^{7-}$ , respectively, and taking into account the identity  $S_{iz} = P_{i1} - P_{i,-1}$ , we obtain the expression

$$\hat{V} = V \sum_{\langle ij \rangle} S_{iz} S_{jz} + 4V q_0 \sum_i S_{iz} + 2NV q_0^2,$$

which differs from (1) only in the shift of the energy and chemical potential reference levels.

Thus, the system can be diluted by charged impurities which are mobile and can enter the charge–charge interaction. The properties of the system in the ground state were studied in the mean-field approximation [15]. Then, the mean-field approximation [16] and the Bethe approximation [17] were used to obtain the temperature phase diagrams and the thermodynamic characteristics. The introduction of a charge disorder in the model can also substantially influence the critical behavior and phase states of the spin systems [18, 19]. However, the aim of this work is to study the influence of the competition of two interactions on the formation of the ground state of an Ising magnet; thus, we consider only the case  $n = 0$ .

The numerical simulation of the spin–pseudospin system was performed using the classical Monte Carlo (MC) method. The common Metropolis algorithm was modified [20] for the charge density (2) fixation to be possible at each MC step, and also it was parallelized using the CUDA technology. The MC calculations were performed on a square lattice with periodic boundary conditions, linear sizes  $La$ , the number of sites  $N = L \times L$ , where  $a$  is the lattice parameter taken as 1. All calculations were carried out simultaneously for a hundred copies of the system, to

refine the results and also to analyze the behavior of the system near the frustration.

The temperature dependences of the specific heat and (pseudo-)magnetic susceptibility are determined using the fluctuation relationships

$$\begin{aligned} C &= \left( \frac{\partial E}{\partial T} \right)_H = \frac{1}{N} \frac{\langle E^2 \rangle - \langle E \rangle^2}{k_b T^2}; \\ \chi &= \left( \frac{\partial \mathcal{O}}{\partial H} \right)_T = \frac{1}{N} \frac{\langle \mathcal{O}^2 \rangle - \langle \mathcal{O} \rangle^2}{k_b T}, \end{aligned} \quad (3)$$

where  $k_B$  is the Boltzmann constant,  $E$  is the energy of the system with Hamiltonian (1). Order parameter  $\mathcal{O}$  for the checkerboard antiferromagnetic ( $m$ ) and charge-ordered ( $M$ ) phases characterizes the spontaneous orientation ordering of the system of pseudospins and is determined as follows:

$$\mathcal{O} = \begin{cases} m = m_1 - m_2, \\ M = M_1 - M_2. \end{cases} \quad (4)$$

Here,  $m_\lambda = \sum_{i \in \lambda} s_{iz}$  is the magnetization of sublattice  $\lambda = 1, 2$ , and  $M_\lambda = \sum_{i \in \lambda} S_{iz}$  is the mean charge of sublattice  $\lambda$  (pseudo-magnetization).

The critical temperatures of phase transitions (PT) were determined by the maxima of the specific heat and the susceptibility and also were checked using the Binder cumulant method [21].

### 3 Results and discussion

Figure 1 depicts the temperature phase diagrams in the dependence on the single-ion anisotropy parameter  $\Delta/J$  for various ratios between the exchange interactions  $V/\tilde{J}$ . The phase diagrams have a characteristic shape of “checkmarks”, in the right part of which the system is transformed from the non-ordered (NO) paramagnetic state to the antiferromagnetic ordered (AFM) state of spins  $s = 1/2$ , while, in the left part, it is transformed to the staggered charge order (CO) of pseudospins  $S = 1$  (except for the case  $V/\tilde{J} = 0$ , when the charge order is impossible). At the

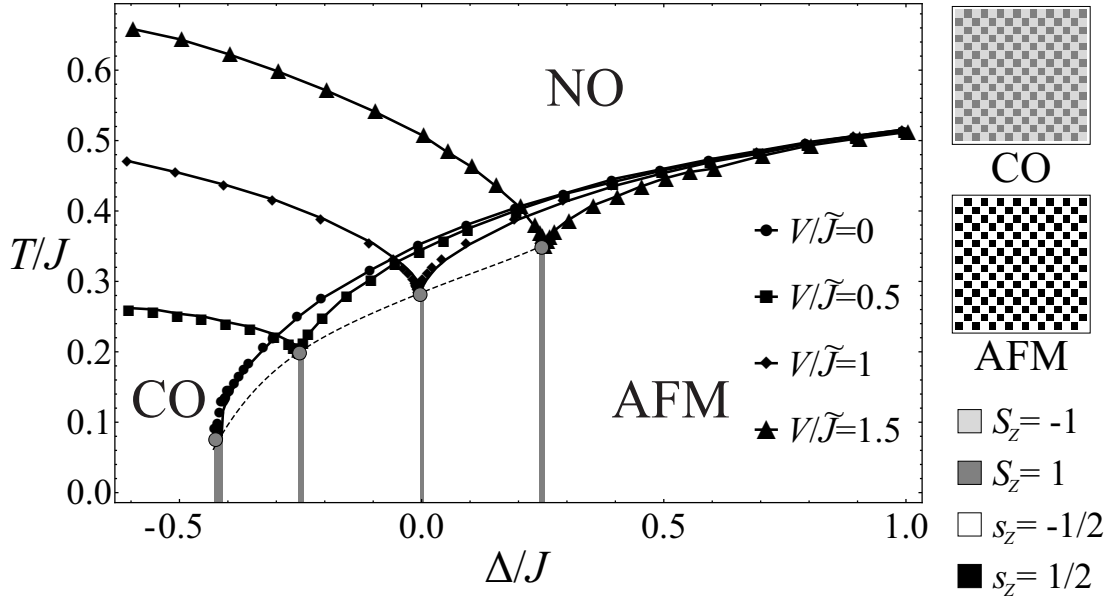


Figure 1: Temperature phase diagrams obtained in the absence of doped charge ( $n = 0$ ) for  $V/\tilde{J} = 0, 0.5, 1$  and  $1.5$ . The grey points indicate the position of the frustration point  $\Delta^*$ . The grey vertical bands correspond to the frustration areas for every  $V/\tilde{J}$  ratio

boundary between these two phases, the ground state of the system is degenerate because of the competition between charge and magnetic orderings. In this system, singleion anisotropy parameter  $\Delta/J$  is a frustrating one, and the point at which the type of ordering in the ground state is changed determines the frustration point  $\Delta^*$ . This point is a classic analog of the quantum critical point. This type of the phase diagrams of the frustrated systems is widely distributed in the literature and, for example, it is represented by the Ising model with the competing interaction between the nearest and nextnearest neighbors on bcc or simple cubic lattices [22, 23]. However, such phase diagrams were obtained for the first time for the model with mixed spin  $s = 1/2$  and pseudospin  $S = 1$ .

A change in the ratio between the exchange interactions leads to a shift of the frustration point  $\Delta^*$  to larger  $\Delta/J$ , and this point becomes zero at  $V = \tilde{J}$ ; the temperature phase diagram becomes symmetric with respect to line  $\Delta^* = 0$ . Thus there is a boundary between the cases of strong ( $V \leq \tilde{J}$ ) and weak ( $V > \tilde{J}$ ) spin exchanges. This boundary leads to qualitative distinctions between the  $\Delta/J - n$

diagrams of the ground state, and also to other effects observed as the fixed charge density  $n$  increases, as described in [15, 19].

It is suggested that such phase diagrams have only one frustration point corresponding to the minima of the dependences of the PT temperature on the frustrating parameter. However, we revealed that the ground state is degenerate in a whole “frustration area”, rather than in one specific point. In this range, both charge and antiferromagnetic orderings form in the ground state with nonzero probabilities. This implies that, with identical model parameters and thermalization conditions, a part of copies of the system is ordered antiferromagnetically and another part has the charge ordering. These areas are denoted by grey vertical lines in Fig. 1.

Figure 2 shows the dependences of the probabilities of formation of the CO and AFM types of ordering for various ratios  $V/\tilde{J}$  on the frustrating parameter  $\Delta/J$ . The calculations were performed for 100 copies of the system with linear lattice sizes  $L = 128$  and also verified for  $L = 192$ . Far from the frustration point, the ground state is determined exactly: either the CO order or the AFM order form. However, when approaching the frustration point, the energies of these phases become the same, and both the CO phase and AFM phase can form in some copies of the system. Thus, the frustration point will be the value of parameter  $\Delta/J$ , at which both the phases are equally probable in the ground state. We will call the area around the frustration point in which the probabilities of formation of both the phases are nonzero, the frustration area (grey areas in Figs. 1 and 2).

The competition of charge and spin interactions leads not only to the degeneracy of the ground state but also to the change in the type of PT. Figure 3 shows the temperature dependences of the order parameters of AFM ( $m$ , black curves) and CO ( $M$ , grey curves) order parameters for several various copies of the system obtained at the same parameters  $L = 128$ ,  $V/\tilde{J} = 4$ ,  $\Delta/J = 1.455$ . In this case, the dependences of the CO parameter  $M$  behave sharper than the dependences of the AFM parameter  $m$ ; thus, we additionally performed the analysis of the energy

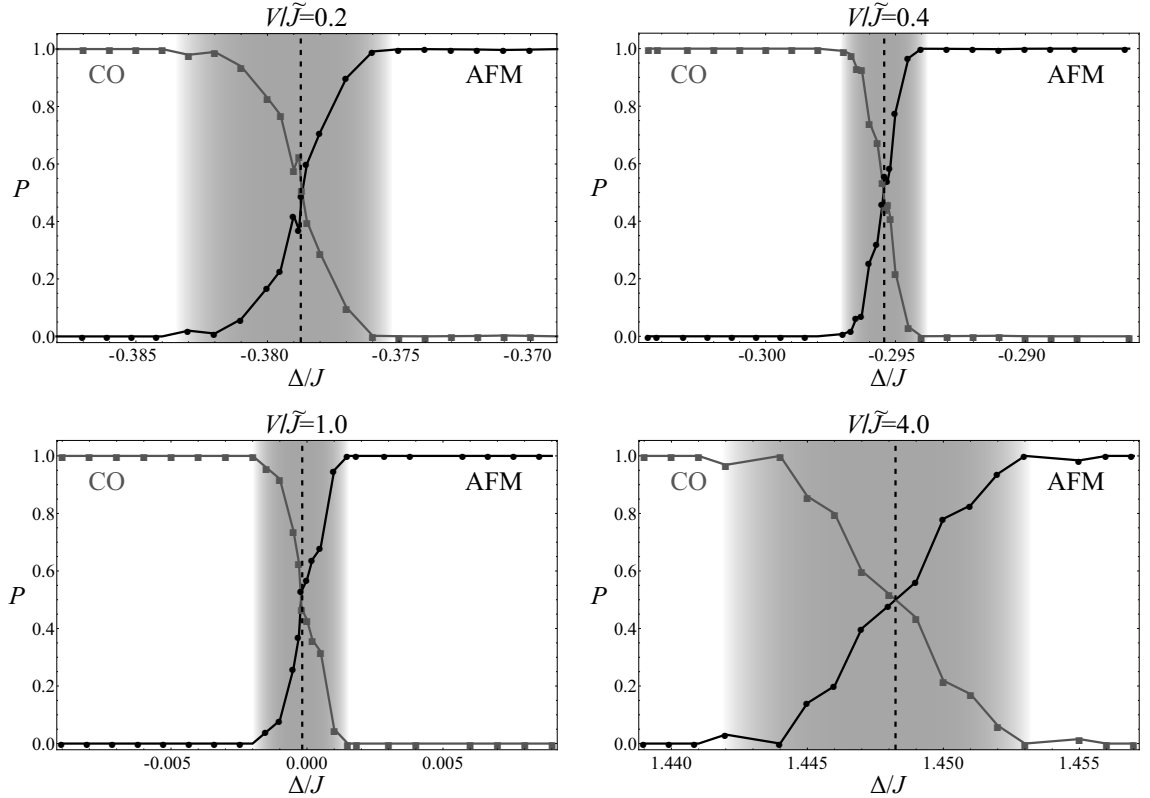


Figure 2: Distribution of the probabilities of the formation of AFM (black curve) and CO (grey curve) types of ordering in the ground state near the frustration point for  $V/\tilde{J} = 0.2, 0.4, 1, \text{ and } 4$ . The grey color shows the areas in which the probability of detecting both phases in the ground state is nonzero.

histograms [24, 25], which allows us to determine the PT type with a high reliability. For a first-order PT, the histogram of energy distribution  $P(E)$  near the critical temperature  $T_c$  must have a two-peak structure, each peak of which corresponds to a certain (stable or metastable) phase, which is demonstrated by a stepwise change in the energy. In the case of a second-order PT, the histogram will have the form of the normal distribution, where the most probable value of the energy corresponds to the equilibrium value of the energy of one phase at given temperature.

Figure 4 shows the histograms of the energy distribution  $\varepsilon = E/(NJ)$  by the MC steps for copy 1 with charge ordering and for copy 2 ordered antiferromagnetically (Fig. 3). The histograms are built near the critical point at  $T = 0.5255J$ . The data binning was performed over 1000 ranges for  $2 \cdot 10^6$  MC steps. The energy distribution over MC steps is built in the inset.



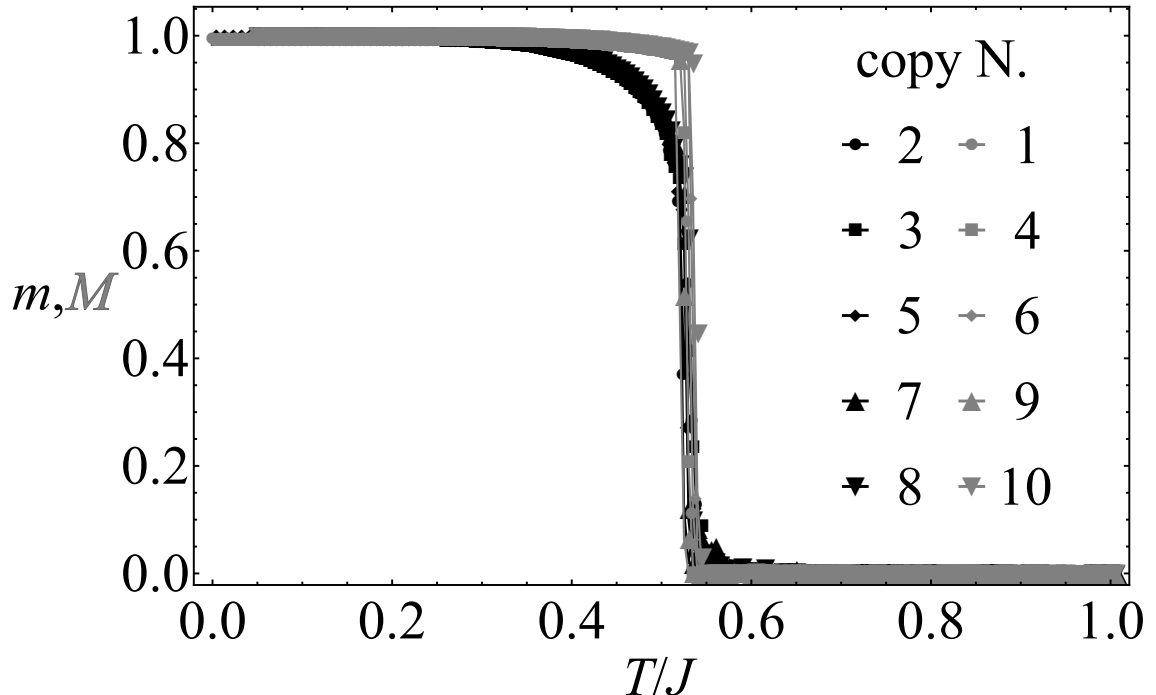


Figure 3: Temperature dependences of order parameters  $m$  (black curves) and  $M$  (grey curves) for ten various copies of the system at  $L = 128$ ,  $V/\tilde{J} = 4$ , and  $\Delta/J = 1.455$ . A part of the copies transits to the AFM state, and another part transits to the CO state.

The existence of two peaks in the histogram of the energy distribution demonstrates that the transition to the CO state in copy 1 is the first-order phase transition. The peak with a higher energy corresponds to the non-ordered phase, and the peak with lower energy corresponds to the charge order. One pronounced maximum in the energy distribution histogram for copy 2 shows that there is the second-order PT to the AFM state.

The further analysis of the energy histograms for various  $V/\tilde{J}$  showed that, in the case of a weak spin exchange ( $V/\tilde{J} > 1$ ), the transition to the CO state near the frustration point is the first-order PT and the transition to the AFM state is the second-order PT. In this case, the region width with the first-order PT becomes larger with an increase in the  $V/\tilde{J}$  ratio and the distance from point  $V/\tilde{J} = 1$ . In the case of the strong spin exchange  $V/\tilde{J} \leq 1$ , the opposite situation is observed: the transition to the AFM state near the frustration point is the first-order PT and the transition to the CO phase is the second-order PT. In this case, the width of

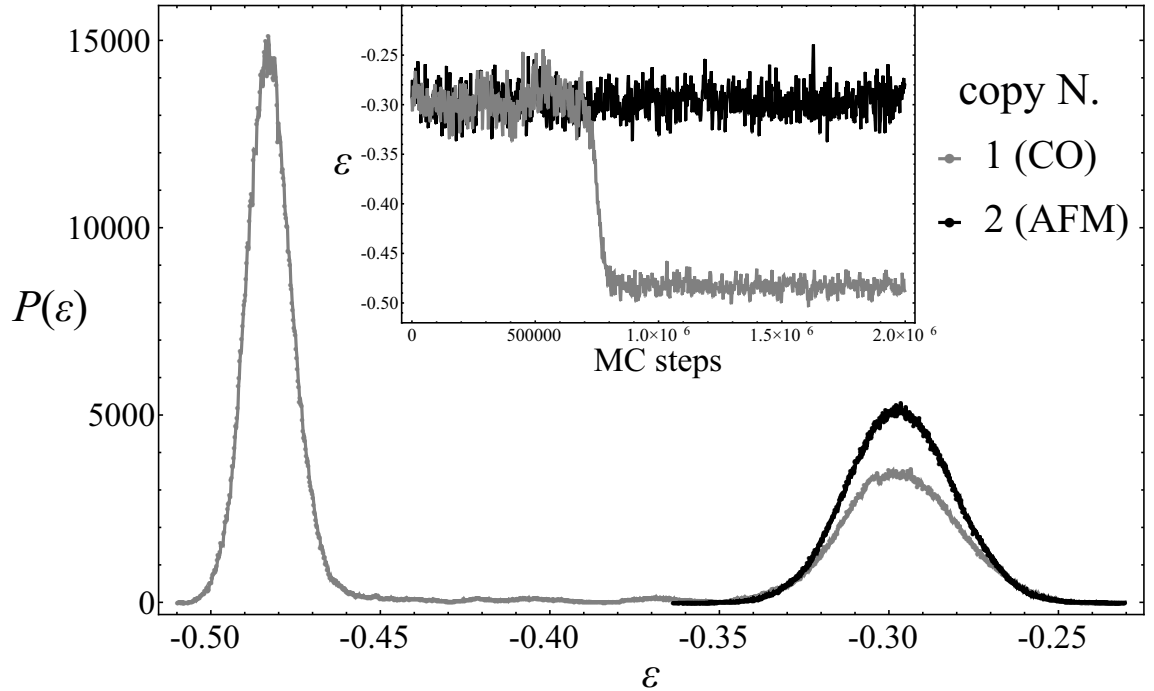


Figure 4: Histograms of the energy distribution  $\varepsilon = E/(NJ)$  for two copies of the system with parameters  $L = 128$ ,  $V/\tilde{J} = 4$ , and  $\Delta/J = 1.455$  at temperature  $T = 0.5255J$ . The two-peak structure of the histogram for copy 1 (grey color) demonstrates the first-order PT to the CO state. Single-peak Gaussian histogram for copy 2 (black color) shows the second-order PT to the AFM state.

the region with the first-order PT increases as the distance from point  $V/\tilde{J} = 1$  increases and as the  $V/\tilde{J}$  ratio decreases.

## 4 Conclusions

The peculiarities of the ground state and the phase transitions of the spin–pseudospin model of a twodimensional magnet with the frustration, caused by the competition of charge and magnetic orderings have been studied using the classical Monte Carlo method. It is shown that near the frustration point, there is an area in which the probabilities of the formation both charge and antiferromagnetic phases are nonzero. Thus, the same system can be variously ordered at the same conditions; i.e., the ground state of the system is degenerate in a certain frustration area, rather than in a point.

In addition, based on the histogram analysis of the data, it is found that the frustration influences the types of PT. Near the frustration point in the case of the strong spin exchange, for small  $V/\tilde{J}$ , the system undergoes the first-order PT to the AFM state, and, in the case of a weak spin exchange, for large  $V/\tilde{J}$ , to the CO state.

## 5 Acknowledgements

The authors are grateful to A.S. Moskvin for stimulating discussions.

## 6 Funding

This work was supported by the Competitiveness Enhancement Program of the Ural Federal University (Act 211 of the Government of the Russian Federation, Agreement no. 02.A03.21.0006 and CEP 3.1.1.1.g-20) and the Ministry of Science and Higher Education of the Russian Federation (project FEUZ-2020-0054).

## References

- [1] E. Fradkin, S. A. Kivelson, and J. M. Tranquada, *Rev. Mod. Phys.* **87**, 457 (2015).
- [2] A. S. Moskvin, *Phys. Rev. B* **84**, 075116 (2011).
- [3] A. S. Moskvin, *J. Phys.: Conf. Ser.* **592**, 012076 (2015).
- [4] Y. D. Panov, A. S. Moskvin, A. A. Chikov, and I. L. Avvakumov, *J. Supercond. Nov. Magn.* **29**, 1077 (2016).
- [5] M. Blume, V. J. Emery, and R. B. Griffiths, *Phys. Rev. A* **4**, 1071 (1971).
- [6] K. E. Newman and J. D. Dow, *Phys. Rev. B* **27**, 7495 (1983).
- [7] J. Sivardi ere and J. Lajzerowicz. *Phys. Rev. A* **11**, 2101 (1975); *Phys. Rev. A* **11**, 2090 (1975).

- [8] C. C. Loois, G. T. Barkema, and C. M. Smith, Phys. Rev. B **78**, 184519 (2008).
- [9] S. A. Cannas and D. A. Stariolo, Phys. Rev. E **99**, 042137 (2019).
- [10] *Frustrated Spin Systems*, Ed. by H. T. Diep, 2nd ed. (World Scientific, Singapore, 2013).
- [11] T. A. Kaplan and N. Menyuk, Philos. Mag. **87**, 3711 (2007).
- [12] A. Kalz and A. Honecker, Phys. Rev. B **86**, 134410 (2012).
- [13] L. Balents, Nature (London, U.K.) **464**, 199 (2010).
- [14] S. T. Bramwell and M. J. P. Gingras, Science (Washington, DC, U. S.) **294**, 1495 (2001).
- [15] Y. D. Panov, A. S. Moskvina, A. A. Chikov, and K. S. Budrin, J. Low Temp. Phys. **187**, 646 (2017).
- [16] Yu. D. Panov, V. A. Ulitko, K. S. Budrin, D. N. Yasinskaya, and A. A. Chikov, Phys. Solid State **61**, 707 (2019).
- [17] Yu. D. Panov, A. S. Moskvina, V. A. Ulitko, and A. A. Chikov, Phys. Solid State **61**, 1627 (2019).
- [18] D. N. Yasinskaya, V. A. Ulitko, A. A. Chikov, and Y. D. Panov, Acta Phys. Polon. A **137**, 979 (2020).
- [19] D. N. Yasinskaya, V. A. Ulitko, and Yu. D. Panov, Phys. Solid State **62**, 1713 (2020).
- [20] K. S. Budrin, V. A. Ulitko, A. A. Chikov, Y. D. Panov, and A. S. Moskvina, in *Proceedings of the Conference on Parallel Computational Technologies PCT'2018* (2018), p. 22.
- [21] K. Binder and D. W. Heermann, *Monte Carlo Simulation in Statistical Physics* (Springer, Berlin, 1992).
- [22] A. K. Murtazaev, M. K. Ramazanov, F. A. KassanOgly, and D. R. Kurbanova, J. Exp. Theor. Phys. **120**, 110 (2015).
- [23] M. K. Ramazanov and A. K. Murtazaev, Phase Trans. **91**, 83 (2018).

[24] F. Wang and D. P. Landau, Phys. Rev. Lett. **86**, 2050 (2001).

[25] A. M. Ferrenberg and D. P. Landau, Phys. Rev. B **44**, 5081 (1991).